



Application of groundwater functional zoning to coastal groundwater management: a case study in the plain area of Weifang City, China

Xu Guo¹ · Chuanming Ma¹ · Xinjie Hu¹ · Xiaojing Hu¹ · Wu Yan¹

Received: 1 July 2018 / Accepted: 3 August 2019 / Published online: 14 August 2019
© Springer-Verlag GmbH Germany, part of Springer Nature 2019

Abstract

As a useful index-based evaluation framework, groundwater functional zoning (GWFZ) presents a very positive effect on groundwater management at a regional scale due to its concise results. Currently, the GWFZ lacks definition and detailed processes, hence requiring a systematic structure to offer more knowledge bases to the methodology. A typical study area (Weifang City) characterized by a coastal zone and relying on groundwater supply, as well as the occurrence of groundwater-derived geo-environmental issues, was chosen. We provided a detailed index-based GWFZ method by focusing on the assessment of the resource supply function (RSF) and geo-environment stability function (GSF), with a good understanding of the hydrogeological conditions in the selected area. The RSF was assessed by delineating the potential area of groundwater exploitation, while the GSF was evaluated by identifying the vulnerability of geo-environmental issues. By integrating the RSF and GSF into the GIS environment, the study area was finally divided into five functional sub-areas: concentrated groundwater supply area (1.08%), decentralized groundwater supply area (18.36%), vulnerable geo-environment area (11.78%), unsuitable to exploit groundwater area (14.11%), and recharge protection area (54.67%). Seven groundwater exploitation boreholes in the plain area were validated to be unreasonable with regard to mining scale, which indicates a connection with the inland saltwater intrusion boundary in recent years. With simple data acquisition methods and concise results, GWFZ is of great benefit to groundwater management and can be further applied in other regional studies.

Keywords Groundwater functional zoning · Coastal area · Groundwater management · Geographic information system · Geo-environmental issues · Vulnerability assessment

Introduction

Groundwater plays a vital role as a source of decentralized drinking water for millions of rural and urban households (Kumar and Shah 2006). However, in northern China, over-exploitation of groundwater resources in coastal areas has

already caused a series of large-scale groundwater depression cones, which are continuing to expand in some regions, accompanied by serious geo-environmental issues such as seawater/saltwater intrusion SWI and land subsidence (LSD) (Li and Wu 2010).

Therefore, it is of great practical significance to carry out groundwater management on a regional scale. To achieve this aim, Adiat et al. (2012) presented the spatial prediction of potential zones of sustainable groundwater resources in Malaysia using GIS and multi-criteria decision analysis (MCDA) as spatial prediction tools. In detail, drainage density, lineament density, lithology, rainfall and slope were the main considerations influencing the groundwater storage potential of the area. Similarly, an indicator-based framework combined with the RS, the GIS and MCDA techniques for delineation of groundwater potential zones provided the groundwater sustainability in the Durg district (Kumar et al. 2014). However, the differences in hydrogeological context not only determine the discrepancy in the potential

This article is a part of Topical Collection in Environmental Earth Sciences on Water Sustainability: A Spectrum of Innovative Technology and Remediation Methods, edited by Dr. Derek Kim, Dr. Kwang-Ho Choo, and Dr. Jeonghwan Kim.

Electronic supplementary material The online version of this article (<https://doi.org/10.1007/s12665-019-8534-3>) contains supplementary material, which is available to authorized users.

✉ Chuanming Ma
machuanming@cug.edu.cn

¹ School of Environmental Studies, China University of Geosciences, Wuhan 430074, China

of groundwater storage, but also the differences in impact on the geo-environment during groundwater exploitation. For instance, Chachadi (2005) inferred that the continuous anthropogenic interference in the coastal hydrological and hydrogeological regimes has resulted in pollution of coastal aquifers by SWI. Thus, they defined SWI vulnerability as “the sensitivity of coastal groundwater to SWI due to an imposed groundwater pumping or sea level rise or both, which is determined by the intrinsic characteristics of the aquifer” and proposed an indicator-based model computed in the GIS environment for identifying the spatial distribution of SWI vulnerability.

Overall, constructing an indicator-based framework combined with the MCDA technique and computing a comprehensive index (CI) by overlaying indicator maps in the GIS environment is becoming one of the most widely used methods for groundwater management (e.g., Singh et al. 2018; Adiat et al. 2012; Kumar et al. 2014; Wang et al. 2012; and Mogaji and Lim 2018). However, although the aforementioned researchers presented useful knowledge based on groundwater management, there are still few frameworks that comprehensively consider the factors influencing the groundwater exploitation. In recent years, groundwater functional zoning (GWFZ), which was developed by Dong et al. (2013), has provided a realistic method pertaining to the comprehensive guidance of groundwater exploitation. They divided Tianjin city into seven functional sub-areas

(i.e., central water supply zones for urban area, non-central water supply area in built-up area, land subsidence area, salt water area, etc.) by considering 12 indicators, such as supply conditions, water abundance, hydrogeological conditions, water quality, protection targets, and the present situation of groundwater exploitation. The results of GWFZ clearly presented strategies for regional groundwater management, whereas the lack of definition and detailed processes in GWFZ make the results somewhat ambiguous, hence requiring a systematic structure to offer more knowledge bases to the methodology. As shown in Fig. 1, recharge is the amount of renewable resources in the aquifer. In addition, the amount of human exploitation should not exceed the recharge to avoid the depletion of groundwater resources in aquifers. To achieve the sustainable use of groundwater resources, pumping groundwater from aquifers should be less than the recharge while avoiding the geo-environmental issues caused by the water table depression during the process of exploitation (Zhang et al. 2011). Therefore, GWFZ can be assessed by selecting indicators from two aspects according to the specific hydrogeological context.

1. The resource supply function (RSF) emphasizes the delineation of the potential area of groundwater exploitation in the study area.
2. With regard to the geo-environment stability function (GSF), the essential characteristics of aquifers are used

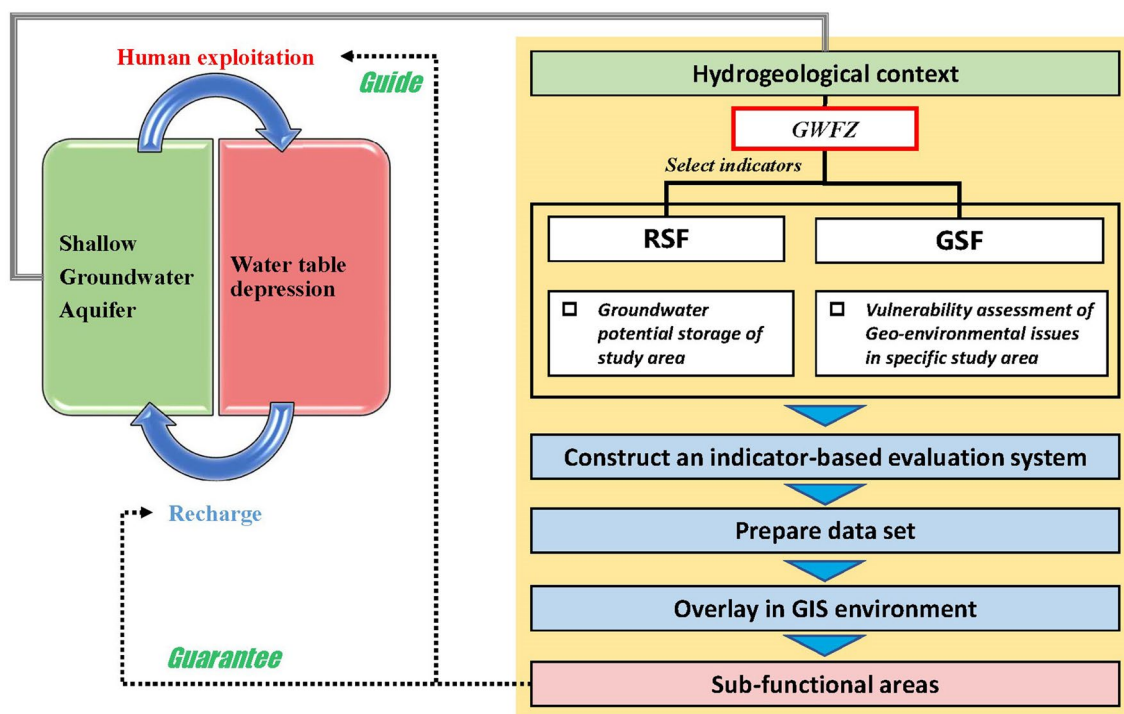


Fig. 1 How GWFZ works for groundwater management

to identify the vulnerability to geo-environmental issues, and the results can be utilized to evaluate GSF.

In this paper, a coastal area (Weifang City) was selected as the study area. We constructed an indicator-based system focusing on the RSF and GSF with a good understanding of the hydrogeological conditions in the study area. Moreover, the results of GWFZ can be obtained in the GIS environment by integrating the RSF and GSF. For instance, concentrated groundwater supply areas are characterized by good RSF and GSF, and areas with poor GSF should be divided into vulnerable geo-environment areas. The main objective of this study is to provide an improved and more detailed GWFZ that can contribute to the management and rational exploitation of groundwater resources; furthermore, this method can be applied to other regions in the world.

Materials and methods

Study area

The study area (Weifang City) is located in southern Laizhou Bay, at a latitude of 35°42′–37°26′N, and a longitude of 118°10′–120°01′E, and has a total area of 15,859 km² (Fig. 2). The elevation of the study area is high in the south and low in the north. There are five major river systems in

the study area: the Xiaoqing River, Mihe River, Bailanghe River, Weihe River, and Jiaolaihe River from west to east. The annual mean precipitation is 660 mm, which is concentrated in June to August (Chen et al. 1997).

Geology and hydrogeology setting

The study area contains a series of Cretaceous to Quaternary sediments that overlie the Palaeozoic basement. The sedimentary facies of the aquifer change from south to north, from alluvial to proluvial to marine sediments in the plain area. Moreover, the strata in the upper part of the southern proluvial fan are mainly composed of gravel and coarse sandstone, grading into fine sand, silt, sandy clay and silty clay towards the coast (Han et al. 2011). The major shallow aquifers in the study area consist of Quaternary sediments (Fig. 3a, b), with thicknesses of > 10 m in the piedmont area, and gradually down to 3 m towards the coast. Shallow and deep groundwater is unconfined towards the piedmont area, while close to the shoreline, deep groundwater becomes confined because of the increasing emergence of upper sandy clay (Han et al. 2014). The bedrock, which outcrops in the hilly area, is mainly composed of Archaean and Proterozoic metamorphic rock and Cretaceous and Neogene basalt, andesite, trachyte and pyroclastic rock (Han et al. 2014).

Cross-section A–B shows that fresh groundwater in the study area flows from south to north under natural conditions

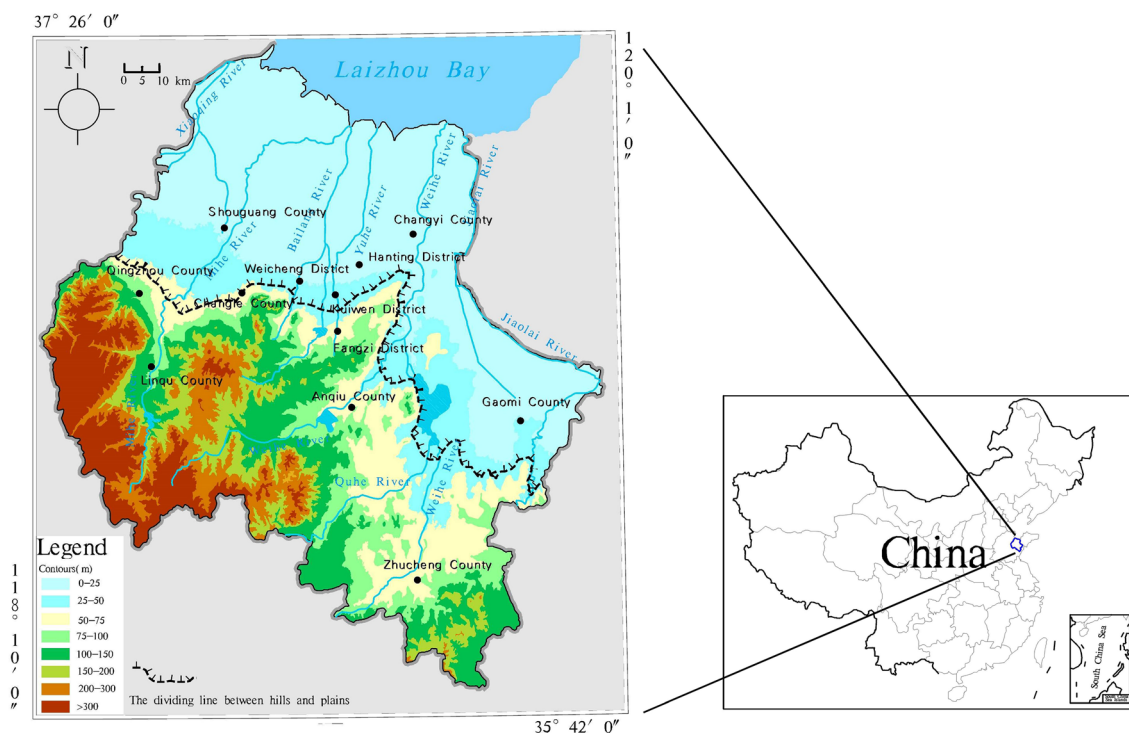


Fig. 2 Location of study area

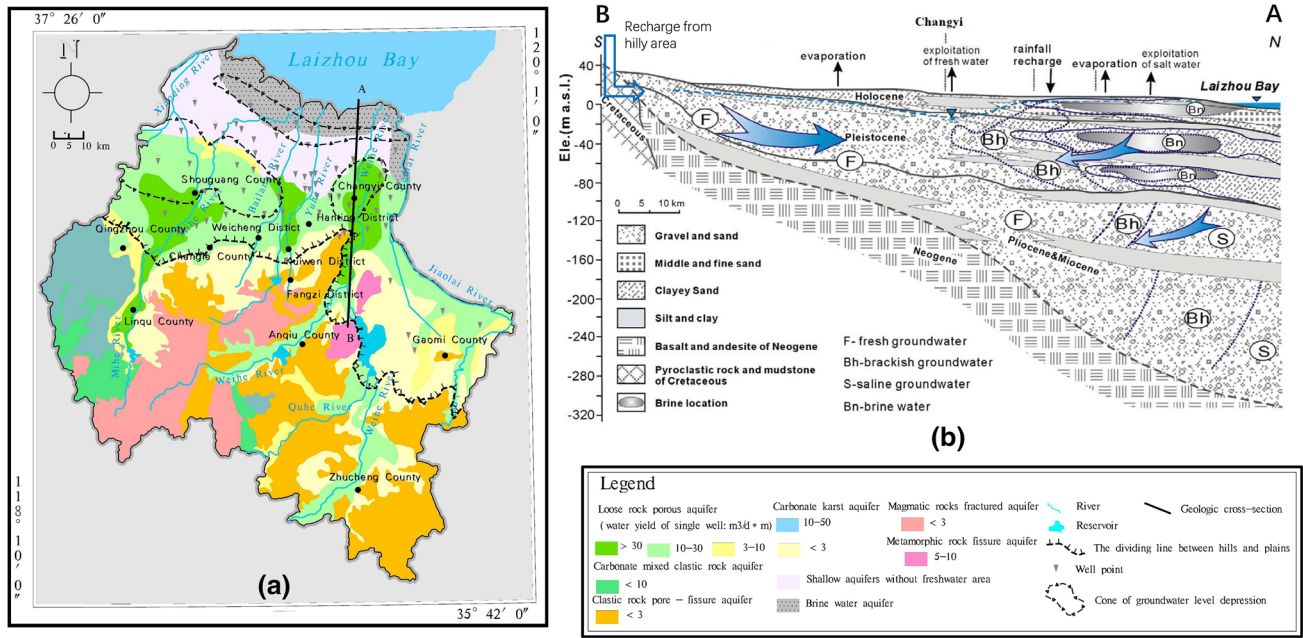


Fig. 3 a Hydrogeological conditions in study area; b cross-section A–B shows the detailed information of hydrogeology (modified by Han et al. 2011)

(Fig. 3b). Figure 3a shows the variation of water abundance in the whole area. From the upper proluvial fan to the edge of the proluvial fan, the water yield of a single well (the well diameter is 219 mm and the drawdown is 5 m) regularly changes from > 30 to < 3 m³/(dm). In terms of fracture aquifers in the hilly area, the water yield of a single well is poor, usually < 10 m³/(dm). With regard to karst aquifers, the water yield appears relatively abundant, i.e., 10–50 m³/(dm). Shallow groundwater aquifers in the plain area are mainly recharged by precipitation, irrigation, horizontal flow of bedrock from hilly areas and vertical infiltration along the

channel. In addition, human exploitation and evaporation are the main discharge ways.

Socio-economical context

Since the 1950s, as shown in Fig. 4a, the urbanization process of the study area has accelerated with the rapid increase in population, from 4.51 million in 1950 to 9.05 million in 2017 (data source: Shandong Statistics Bureau SDSB 2018). Moreover, the growth of the population has led to an obvious increase in the demand for water resources. The

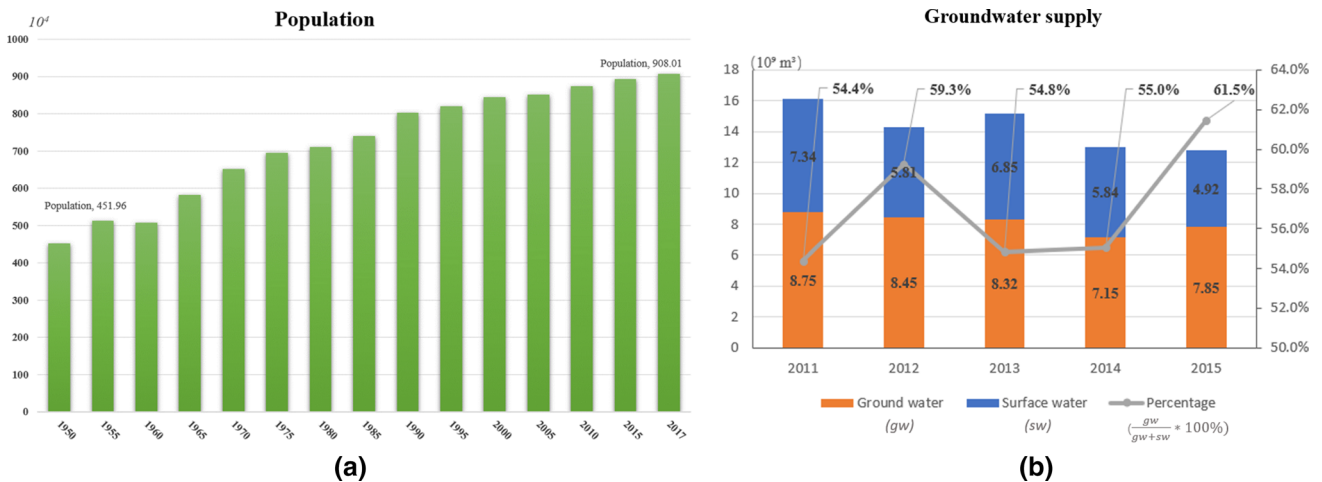


Fig. 4 a Population change from 1950 to 2017; b groundwater is the main source of water supply

per capita water resource in the study area is only approximately 350 m³ (Gao 2005). Groundwater resources, as the main source of water supply, account for more than half of the total water supply for a long time (Fig. 4b). However, the long-term over-exploitation of groundwater exploitation has led to a series of geo-environmental issues, mainly SWI and LSD, especially in the plain area. Changyi County and Shouguang County have formed a large area of groundwater depression cones (Fig. 3a).

The acceleration of urbanization and agricultural development is the main anthropogenic pressures in the study area. In addition, the industrial area is mostly distributed in suburbs of the city, and the cultivated land area accounts for more than 50% of the entire plain area. Since the northern plain area is affected by soil salinization, local residents plant salt-tolerant crops such as corn. Currently, it is necessary and urgent to provide a scientific approach for water management.

Geo-environmental issues

Since the late Pleistocene, three palaeo-seawater intrusions and regressions have occurred along the coast of Laizhou Bay. Brines (defined as TDS > 100 g/L), which exist in Quaternary aquifers, have been found within 10 km of the coastline and at a depth of up to 60 m (Zheng et al. 2014; Guan et al. 2014). The depression cones formed by excessive pumping of both fresh water and brine water in aquifers

have contributed greatly to SWI in the study area. As a result, with increasing hydrostatic pressure on the side of the northern brine area, SWI invades inland continuously (Xue et al. 2000; Guan et al. 2014). Similarly, overexploiting groundwater is the main influencing factor of LSD in coastal areas. Wang et al. (2009) believed that LSD in the northern coastal areas of China mostly occurred in thick layers of loosely consolidated incompressible cohesive soil layers or in normally consolidated layers, depending on the scale of groundwater over-exploitation. The current LSD in the study area is relatively light, concentrated in the center of the depression cones (Fig. 3a), with the development of small ground fissures.

Workflow

As shown in Fig. 5, the process of developing GWFZ is concretely divided into three levels: the functional layer, property layer, and indicator layer. In the GIS environment, the indicator layer is overlaid to obtain the property layer, and then the property layer is superimposed to obtain the function layer. Finally, the functional layer is overlaid to obtain the GWFZ results.

The aforementioned RSF is assessed by delineating the groundwater potential exploitation area. In this paper, the RSF was valued by two property layers: water quantity and water quality. In addition, the main geo-environmental issues in the study area are SWI and LSD. Combined with the

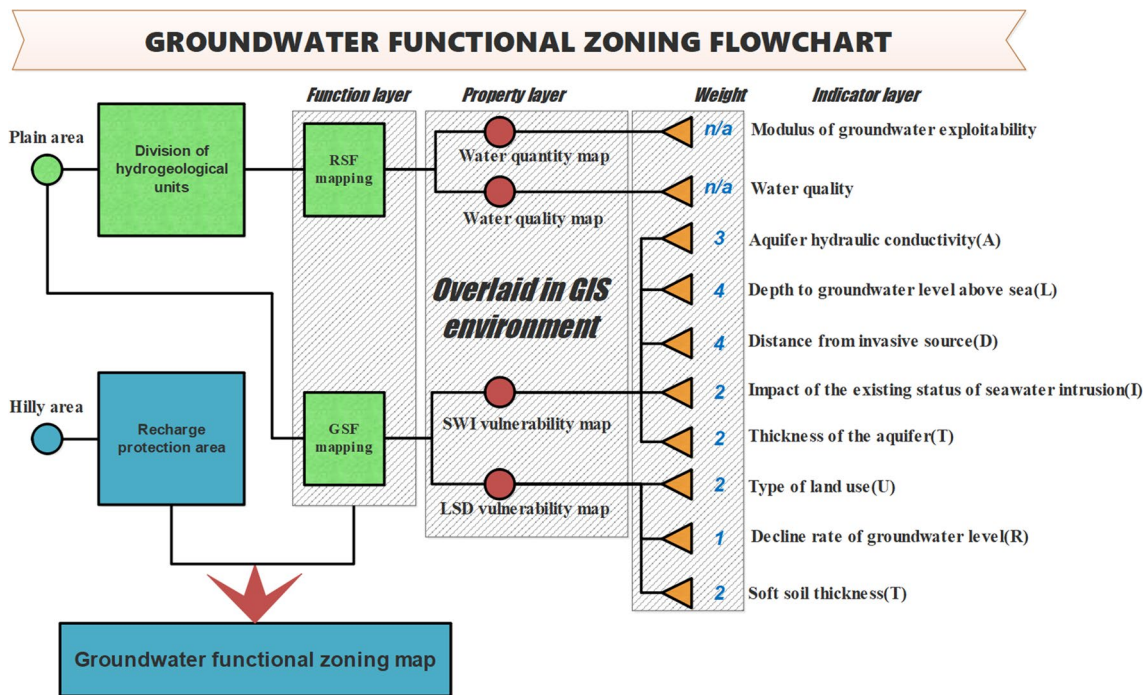


Fig. 5 GWFZ flowchart

hydrogeological context and anthropogenic factors in the study area, we improved the original GALDIT model and the URT model and selected a series of weighted indicators to assess the vulnerability of SWI and LSD.

The flowchart of GWFZ is given in Fig. 5, which includes four sections.

1. Collecting the dataset and preparing an indicator-based framework for GWFZ.
2. Understanding the hydrogeological settings and dividing the study area into several hydrogeological units.
3. Mapping indicator maps and then computing the CI of the property layer by overlaying the indicator maps in the GIS environment.
4. Determining the values of the RSF and GSF by overlaying property layer maps, and then obtaining the results of GWFZ according to the maps of RSF and GSF.

Division of hydrogeological units

Determining the sustainable amount of groundwater exploitation in unconfined aquifers is closely related to the amount of recharge (Zhang et al. 2011). Therefore, when assessing the water quantity in the study area, it is first necessary to identify the evaluation unit characterized by relatively independent recharge sources. The watersheds were used as hydrogeological units for further analysis of water quantity assessment.

In particular, the hilly area is identified as the recharge protection area. This is because all five main rivers in the study area originate from the hilly area, providing a large amount of recharge to the aquifers in the plain area. In addition, the exploitation cost of the fissure aquifer widely distributed in the hilly area is high and the poor single well water yield of the fissure aquifer, are the main considerations. Hydrological analysis is performed based on the acquired DEM data (derived from Google Earth 2018, with a spatial resolution of 10×10 m) in the GIS environment using method of Sun et al. (2008), detailed in Supplementary 1. Five hydrogeological units in the plain area were obtained (i.e., I–V in Fig. 6) (Gao 2005); additionally, shallow aquifers without fresh water (defined as TDS > 1 g/L) were identified and added as the sixth (VI) unit (Fig. 6).

Water quantity assessment

The modulus of groundwater exploitability (MGE) was used to describe the quantity of groundwater in the study area. The MGE is defined as the allowable extraction of groundwater per unit area. The exploitable coefficient method (Gao 2005) was employed to calculate the MGE, as shown in the following equation:

$$\text{MGE} = (\text{TR} \times \rho) / \text{HA}, \quad (1)$$

where the TR is the total recharge of a single hydrogeological unit, ρ is the exploitation coefficient, and HA is the area of a single hydrogeological unit. Additionally, TR consists of precipitation infiltration recharge, irrigation return recharge, lateral runoff recharge and river seepage recharge.

Water quality assessment

From good to poor, the groundwater quality of the analyzed well points can be divided into three levels, i.e., Class III, Class IV and Class V according to the “Groundwater Quality Standard” (MLR 1994). The grading criteria are shown in Table 1.

SWI vulnerability assessment

Vulnerability mapping, especially for SWI, has been widely applied to identify the vulnerable area of SWI using GALDIT model throughout the world (e.g., Chachadi 2005, Motevalli et al. 2018, Recinos et al. 2015, Pedreira et al. 2015, Bouderbala et al. 2016, Luoma et al. 2017, and Allouche et al. 2017). Six indicators are included in this model: Groundwater occurrence (i.e., confined aquifers, unconfined aquifers and leaky confined aquifers.), Aquifer hydraulic conductivity, depth to groundwater above sea Level, Distance from the shore, Impact of the existing status of SWI, and Thickness of the aquifer. The model was modified in this study due to different adaptation conditions from the original model. Concretely, the indicator G was eliminated because the object is shallow groundwater aquifers, and the CI of the modified ALDIT model can be calculated by the following equation after rating and weighting the indicators:

$$\text{CI}_{\text{SWI}} = \left[\sum_{i=1}^5 (W_i R_i) \right] / \sum_{i=1}^5 W_i, \quad (2)$$

where W_i is the weight of each indicator, and R_i is the rating of each indicator. The weights and ratings of the indicators are shown in Table 2.

LSD vulnerability assessment

The LSD is particularly pronounced for the exploitation of groundwater. In China, the hydraulic pressure caused by the exploitation of underground fluids makes the ground compaction a common cause of LSD (Wang et al. 2009). Through an overview of the index-based LSD vulnerability assessment methods, type of land Use, decline Rate of groundwater level, and Thickness of soft soil stratum are the main considerations and determine the LSD vulnerability (e.g., Yang et al. 2013; Zhang et al. 2016; Wang

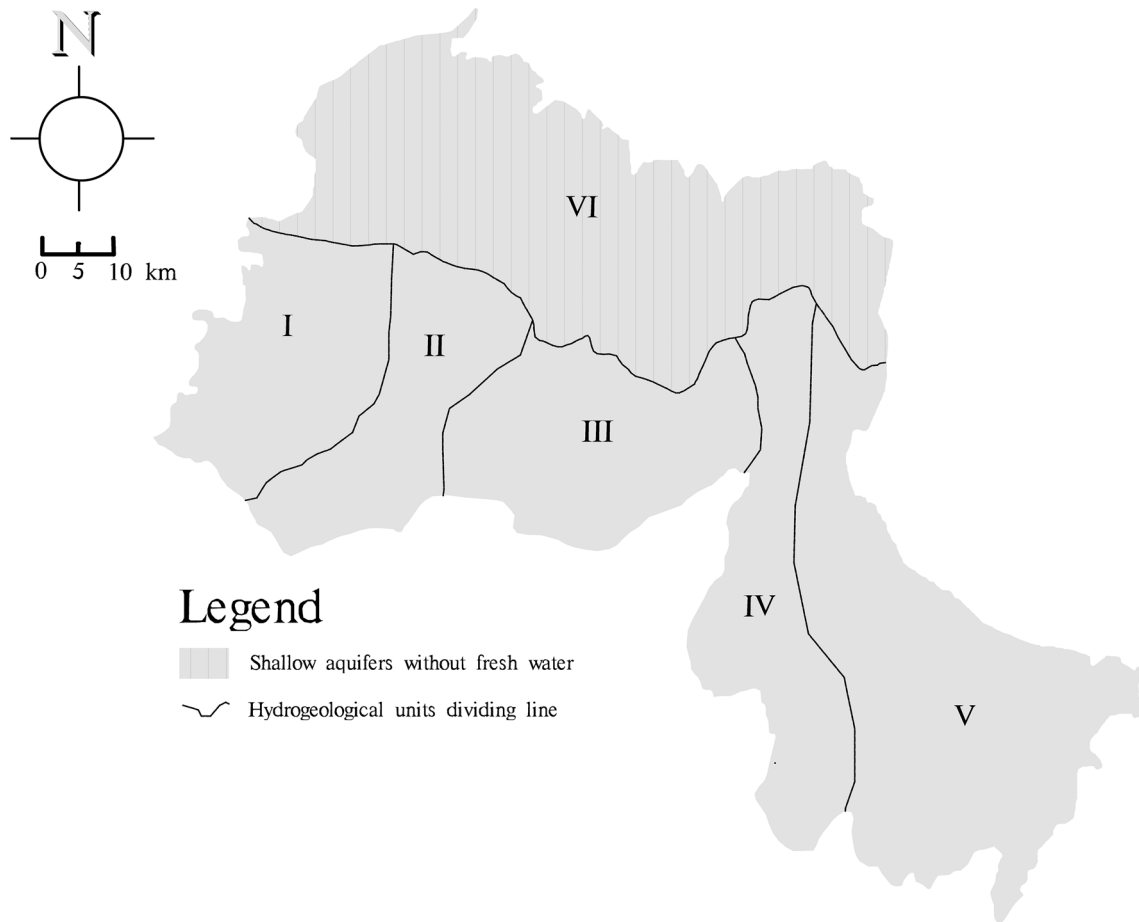


Fig. 6 Six hydrogeological units of the plain area

Table 1 Water quality grading standard

Indicators	Class III	Class IV	Class V
PH	6.5–8.5	5.5–6.5, 8.5–9	<5.5, >9
CaCO ₃ (mg/L)	≤450	≤550	>550
SO ₄ ²⁻ (mg/L)	≤250	≤350	>350
Chloride (mg/L)	≤250	≤350	>350
Fe (mg/L)	≤0.3	≤1.5	>1.5
Mn (mg/L)	≤0.1	≤1.0	>1.0
Cu (mg/L)	≤1.0	≤1.5	>1.5
Zn (mg/L)	≤1.0	≤5.0	>5.0
Phenol (mg/L)	≤0.002	≤0.01	>0.01
Permanganate (mg/L)	≤3.0	≤10	>10
Nitrate (mg/L)	≤20	≤30	>30
Nitrite (mg/L)	≤0.02	≤0.1	>0.1
NH ₄ ⁺ (mg/L)	≤0.2	≤0.5	>0.5
Fluoride (mg/L)	≤1.0	≤2.0	>2.0

et al. 2009; and Hu et al. 2017). Based on the three parameters of the URT model, the CI of LSD vulnerability can be calculated by the following equation:

$$CI_{LSD} = \frac{\sum_{i=1}^3 (W_i R_i)}{\sum_{i=1}^3 W_i} \tag{3}$$

where W_i is the weight of each indicator, and R_i is the rating of each indicator. Table 3 shows the weights and ratings of the indicators.

Results

Results of the indicator layer

In this section, we mainly describe how each indicator affects the property layer and present the acquired data for the indicator layers.

Table 2 Ratings and weights for ALDIT model (modified by Recinos et al. 2015; Pedreira et al. 2015)

Indicator	Weight	Range	Weight ^a	Range ^a	Rating
Aquifer hydraulic conductivity (A)	3	< 5 m/day	3	< 5 m/day	2.5
		5–10 m/day		5–10 m/day	5
		> 10 m/day		> 10 m/day	7.5
Depth to groundwater level above sea level (L)	4	> 2 m	4	> 2 m	2.5
		1.5–2 m		1.5–2 m	5
		1–1.5 m		1–1.5 m	7.5
		< 1 m		< 1 m	10
Distance from the invasive source (D)	4	> 10 km	4	> 30 km	2.5
		5–10 km		15–30 km	5
		2.5–5 km		7.5–15 km	7.5
		< 2.5 km		< 7.5 km	10
Impact of the existing status of SWI (I)	1	< 100 mg/L	2	< 100 mg/L	2.5
		100–250 mg/L		100–250 mg/L	5
		250–500 mg/L		250–500 mg/L	7.5
		> 500 mg/L		> 500 mg/L	10
Thickness of the aquifer (T)	2	< 5 m	2	< 5 m	2.5
		5–7.5 m		5–7.5 m	5
		7.5–10 m		7.5–10 m	7.5
		> 10 m		> 10 m	10

Weight^a and range^a were modified and applied to the SWI vulnerability assessment

Table 3 Ratings and weights for URT model (modified by Yang et al. 2013)

Indicator	Weight	Range	Rating
Land use (U)	2	Town	10
		Village	5
		Other	2.5
Decline rate of groundwater level (R)	1	> 1 m/a	10
		0.2–1 m/a	7.5
		< 0.2 m/a	2.5
Thickness of soft soil stratum (T)	2	> 15 m	10
		10–15 m	7.5
		5–10 m	5
		< 5 m	2.5

Modulus of groundwater exploitability

The study area has a long history of mining groundwater. According to the existing mining data accumulated over the years, Gao (2005) provided the statistical data of recharge amount and exploiting coefficient pertaining to each hydrogeological unit. The MGE of each hydrogeological unit calculated by Eq. 1 are shown in Table 4. In terms of a single hydrogeological unit, $MGE \geq 20,000 \text{ m}^3/\text{km}^2$ satisfies the minimum standard of exploiting groundwater, while $MGE > 100,000 \text{ m}^3/\text{km}^2$ can be used for high-intensity groundwater exploitation (MWR 2005). Figure 7a shows the variation in MGE among the six hydrogeological units.

Table 4 Hydrological units I–VI: MSE was calculated separately

Hydrological units	PIR (10^4 m^3)	RSR (10^4 m^3)	LRR (10^4 m^3)	IRR (10^4 m^3)	TR (10^4 m^3)	ρ	Area (km^2)	MSE ($10^4 \text{ m}^3/\text{km}^2$)
I	5341.91	332.15	152	1400.8	7226.86	0.88	797.3	7.98
II	5050.27	2868.13	984.5	1166.85	10,269.75	0.89	699.3	13.07
III	6696.87	7236.25	2369	1547.29	17,349.41	0.89	927.3	16.65
IV	6212.27	5368.13	1384.5	1435.31	14,700.21	0.89	860.2	15.21
V	13,141.4	694.4	203	744.43	14,783.23	0.9	1693.8	7.85
VI	Shallow aquifers without fresh water							

PIR precipitation infiltration recharge, RSR river seepage recharge, LRR lateral runoff recharge, IRR irrigation return recharge

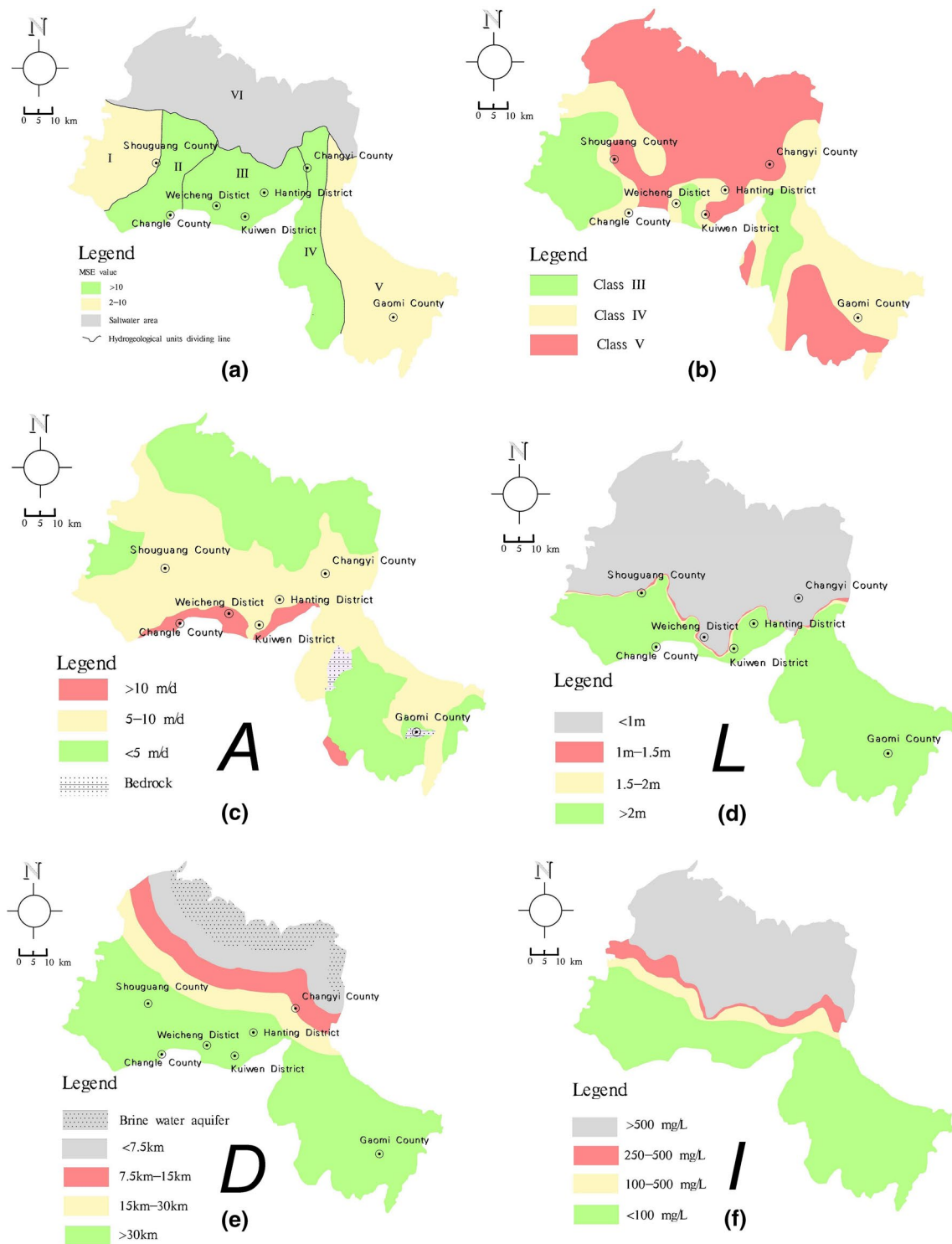


Fig. 7 **a** Distribution of MSE (I–VI), **b** water quality map (modified by Bi 2006); **c–g** indicator maps of ALDIT model; **h–j** indicator maps of URT model

Water quality

From Class III to Class V, the water quality changes from good to poor. Class III water quality is the minimum

standard that meets the demand of drinking water, Class IV is usually used for industrial water demand, and Class V is for agricultural water demand in the study area. Water quality analysis mainly relies on water chemical analysis

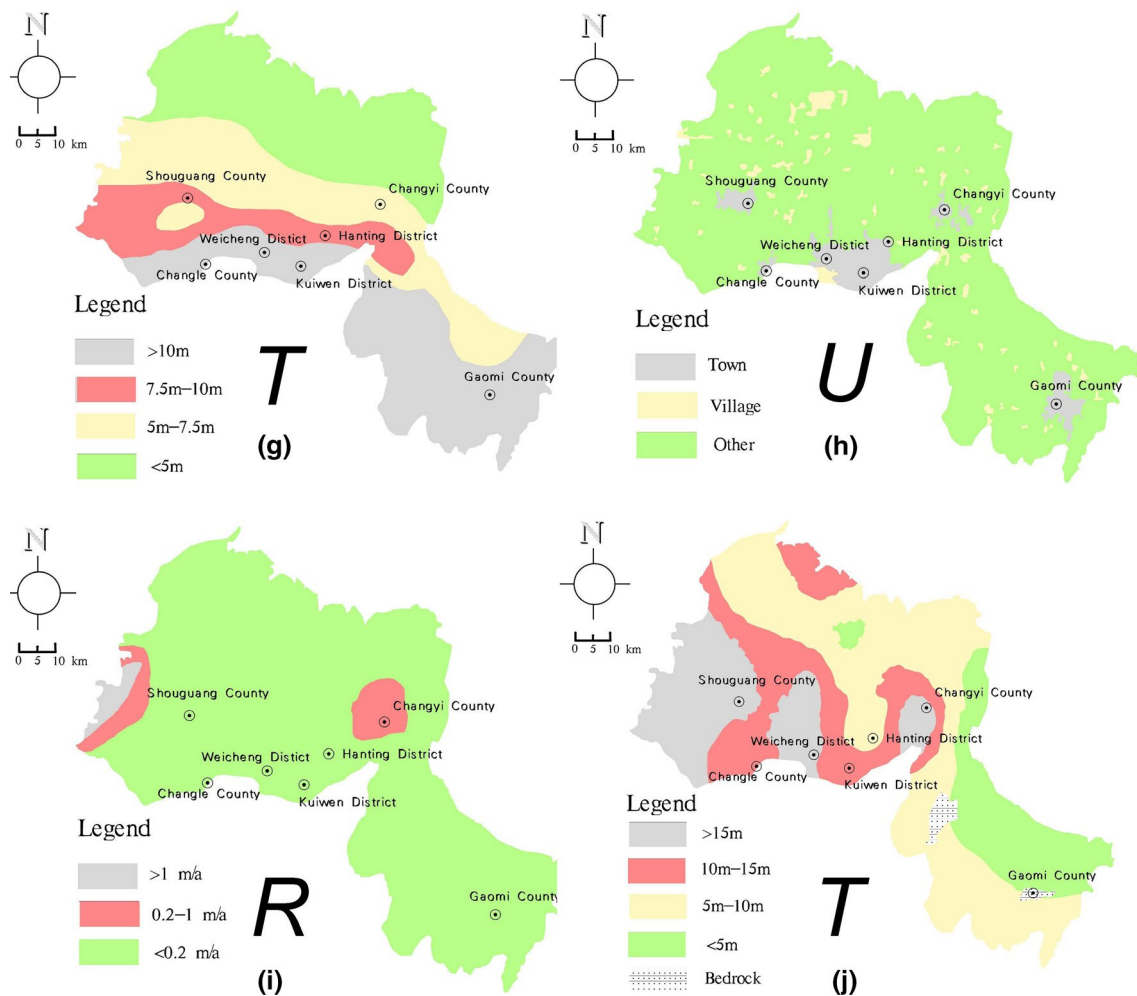


Fig. 7 (continued)

of sampling wells. In this study, the result of a water quality map was provided by Bi (2006). In addition, the spatial distribution of water quality can be obtained in the GIS environment by inputting the water quality results, which can be acquired through comparison with the water quality classification criteria in Table 1. Figure 7b shows the distribution of water quality in the plain area.

Aquifer hydraulic conductivity (A)

The hydraulic conductivity reflects the liquid migration properties of the aquifer and controls the flow velocity of groundwater under a certain hydraulic gradient. The hydraulic conductivity is determined by the porosity and the degree of connectivity among the pores. Under the same hydraulic gradient, a high hydraulic conductivity of an aquifer results in a wider depression cone during the pumping process than low hydraulic conductivity, hence increasing the potential for SWI (Motevalli et al. 2018). In

this study, the spatial distribution of indicator A in Fig. 7c corresponds to the database derived from the China Geological Survey Bureau (CGSB 2017).

Depth to groundwater level above sea level (L)

Depth to groundwater above sea level is a key factor affecting SWI. This parameter determines whether fresh water can remain relatively balanced at the sea water/fresh water interface. The SWI potential is increased when the groundwater level is below sea level, and the lower the water level, the greater the SWI potential is.

In addition, this parameter is calculated by subtracting the depth to the groundwater of the observation wells (available from Zhang et al. 2017 and with a total of 66 observation wells in Fig. 3a) from the altitude of the observation well (Fig. 7d).

Distance from the invasive source (D)

In contrast to previous studies (related to the GALDIT model, e.g., Kazakis et al. 2018 and Mahrez et al. 2018), brine was confirmed to be the major cause of SWI in the study area (Xue et al. 2000; Guan et al. 2014). The distance from the brine aquifer was considered, and parameter D in the GALDIT model was modified to the distance from the invasive source. The partition map can be mapped using the parallel line creation function in GIS (Fig. 7e).

Impact of the existing status of SWI (I)

The impact of the existing status of SWI is regarded as an additional condition for the hydraulic balance of fresh water and salt water (Chachadi 2005). Over-pumping of fresh water, however, has caused the brine water to advance inland, and an undulating salt water/fresh water interface has forming due to exploitation dynamics and the variety of hydrological conditions (Xue et al. 1997, Han et al. 2011). We used the Cl^- ion concentration measured in 2017 as an alternative provided by Zhang et al. (2017) (Fig. 7f). The classification and rating are corresponding to Recinos et al. (2015).

Thickness of the aquifer (T)

The thickness of the aquifer reveals the extent to which the saturated zone can be affected. The thicker the aquifer is, the higher the vulnerability to SWI, and vice versa (Chachadi 2005). The aquifer thickness data (Fig. 7g) were obtained from geological survey and borehole data provided by the CGSB (2017).

Type of land use (U)

This parameter reflects the strength of the surface load. During groundwater pumping, crowded building groups in town area have a greater potential to cause LSD. It is easier to compact the soft soil layer in town areas than in village areas. In addition, taking the high-density population of town areas into account, LSD may cause greater economic losses in town areas than in other areas (Wang et al. 2009). Land use is divided into three categories: town, village and other (Fig. 7h). The land use data were obtained from the database of the CGSB (2017).

Decline rate of groundwater level (R)

Parameter R can directly express the occurrence of negative dynamics of the groundwater system. Using 1 year as the time period, the data on the declining water level of well points was measured, and the results can reveal whether

the exploitation intensity is reasonable. Through statistical analysis of groundwater monitoring data in Shandong Province over the years, the Shandong Hydrology Bureau (SDHB) selected 1357 shallow pore water observation wells, calculated the dynamic rate of groundwater depression during the evaluation period, and produced a water level change rate distribution map. The map of indicator R (Fig. 7i) in the study area was obtained from the database provided by SDHB (2013).

Thickness of soft soil stratum (T)

Due to the long-term over-pumping of aquifers, the upper soft soil of aquifers is compressed by the release of interstitial fluid pressure, hence causing LSD. However, this is an irreversible process. The thicker the soft soil layer, the more easily LSD occurs. Soft soils stratum is defined as soft clay soil and silty soil with a low degree of consolidation, high compressibility, low mechanical strength, and loose structure (Yang 1991). The thickness of a soft soil stratum can be approximately replaced with depth to groundwater in the plain area (which is characterized by loose soil media and a vadose zone upon saturated zone), and can be obtained from selected observation wells (Fig. 7j).

Results of the property layer

Water quantity map

Figure 7a displays the MGE variation of the hydrogeological unit I–VI. The groundwater resources in the study area are abundant. In addition to the northern SWI area, the hydrogeological unit I–V shows good potential for exploitation. In particular, hydrogeological units II, III and IV were identified as having the potential for concentrated large-scale exploitation.

Water quality map

As seen from the Fig. 7b, the areas with poor water quality are mainly concentrated in the center of the city and the suburbs where industry is concentrated. In addition, areas with good water quality are concentrated in the alluvial plains in front of the mountains, especially on the terraces on both sides of the river.

SWI vulnerability map

A total of five indicator maps attributed to the ALDIT model were overlaid in the GIS environment. We calculated the CI of SWI according to Eq. 2 and the standard in Table 2. Based on the criteria in Table 5, SWI vulnerability in the plain area was divided into four categories: very high vulnerability

Table 5 Grading standard for SWI vulnerability

SWI vulnerability	Max: 8.33, Min: 2.83
Low vulnerability	< 4.21
Moderately vulnerability	4.21–5.58
High vulnerability	5.58–6.95
Extremely high vulnerability	> 6.95

areas, high vulnerability areas, moderate vulnerability areas and low vulnerability areas (Fig. 8).

Very high vulnerability areas account for 32.85% of the plain area, and are mainly concentrated in the coastal area. The line Shouguang → Weicheng District → Changyi displays a high-level vulnerability accounting for 16.67% of the plain area. High vulnerability areas are also concentrated in northwest of Changyi County. Overall, high-level SWI vulnerability is mainly characterized by a low groundwater table above sea level (usually < 1 m). Additionally, a short distance from the coast is also an important factor influencing the high vulnerability. In addition, 14.06% of the plain area falls into moderate vulnerability, which is

mainly distributed in the eastern part of Shouguang, Changle County, the eastern part of Kuiwen District and the eastern part of Hanting District. Moderate vulnerability is characterized by a high groundwater table above sea level (usually > 2 m), a moderate distance from the coast, and an aquifer thickness of 5–7.5 m. The low vulnerability areas are mainly distributed in the piedmont alluvial plain far from the coast, accounting for 35.41% of the plain area. These areas are characterized by an aquifer thickness of > 10 m and a relatively high hydraulic conductivity of > 5 m/day. However, the characteristics of a high groundwater table above sea level (usually > 2 m) and a long distance from coastline (> 30 km) significantly contribute to low-level SWI vulnerability.

LSD vulnerability map

Similar to SWI vulnerability, three indicator maps of the URT model were superimposed according to Eq. 3 and the standards provided in Table 6. Figure 9d shows that the LSD vulnerability can be divided into four levels (Fig. 9).

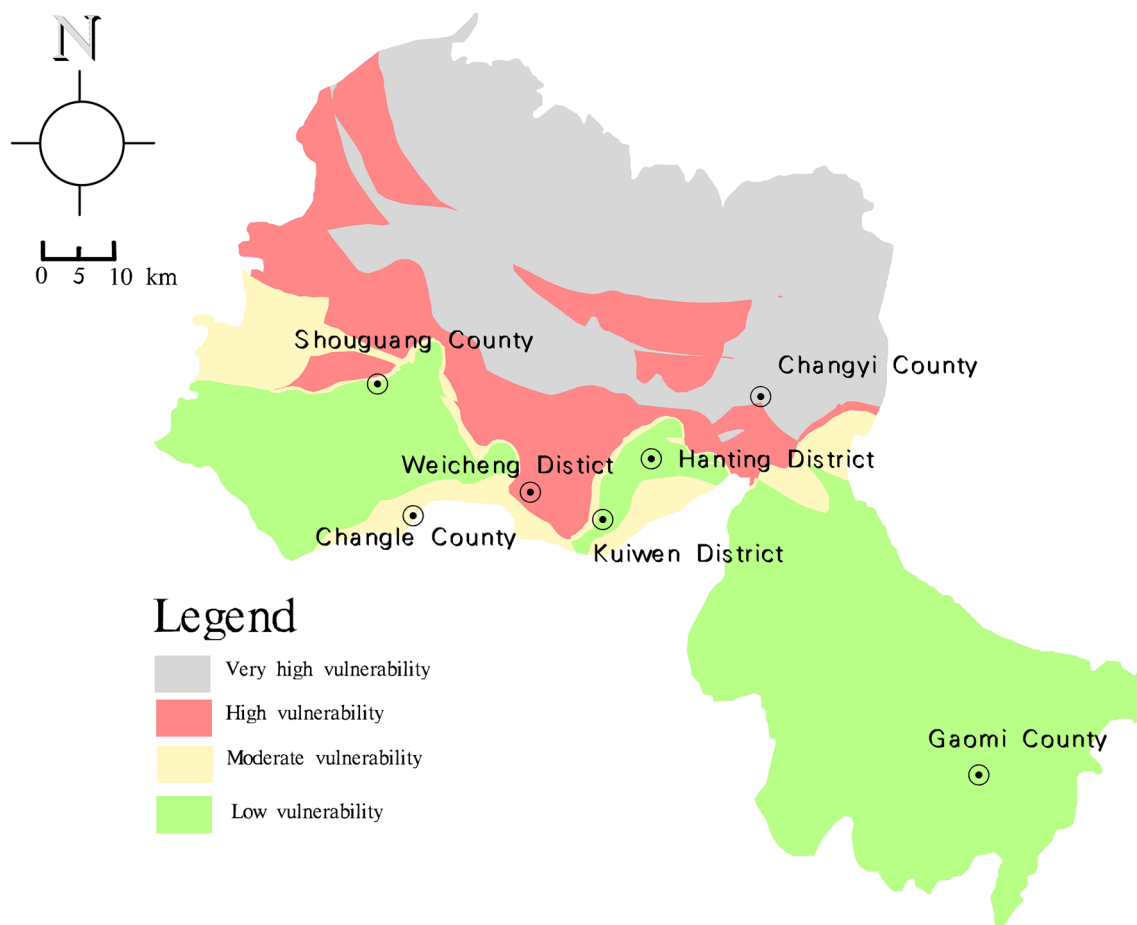
**Fig. 8** SWI vulnerability map

Table 6 Grading standard for LSD vulnerability

LSD vulnerability	Max: 10, Min: 2.5
Low vulnerability	< 4.375
Moderate vulnerability	4.375–6.25
High vulnerability	6.25–8.125
Extremely high vulnerability	> 8.125

Very high and high vulnerability areas account for 19.48% of the entire plain area. These areas are mainly distributed in Shouguang City, Weicheng District and Changyi County. The urban area with dense buildings and high groundwater demands, as well as a large-scale depression cone with a groundwater declining rate of > 0.2 m/year in the eastern part of Shouguang City and Changyi County, exhibits a high-level of LSD vulnerability. The area with moderate vulnerability, accounting for 24.68% of the plain area, is mainly distributed in the suburbs around the urban area. The main characteristics of these areas are the low rates of groundwater decline, and the thickness of soft soil is generally > 10 m. Low-level LSD vulnerability always

occurs in the areas characterized by the thin soft soil layers and sparsely populated regions far from depression cones.

Results of the functional layer

RSF map

The grading standards in Table 7 were used to determine the RSF of six hydrogeological units in the study area (Fig. 10). Close to the piedmont area, the terraces on both sides of the river display good RSF and are characterized by good water quality and high-level MSE. Although Weicheng District and Changyi County all fall into hydrogeological units with high-level MGE, due to high-intensity anthropogenic activities, the groundwater quality in these areas is poor. The large-scale centralized exploitation of groundwater produces a high demand on water quantity and water quality, so these areas are classified into general RSF areas. Moreover, pumping groundwater decreases the groundwater table and forms depression cones, hence changing the regional groundwater flow. For this reason, the SWI area in the northern part of the

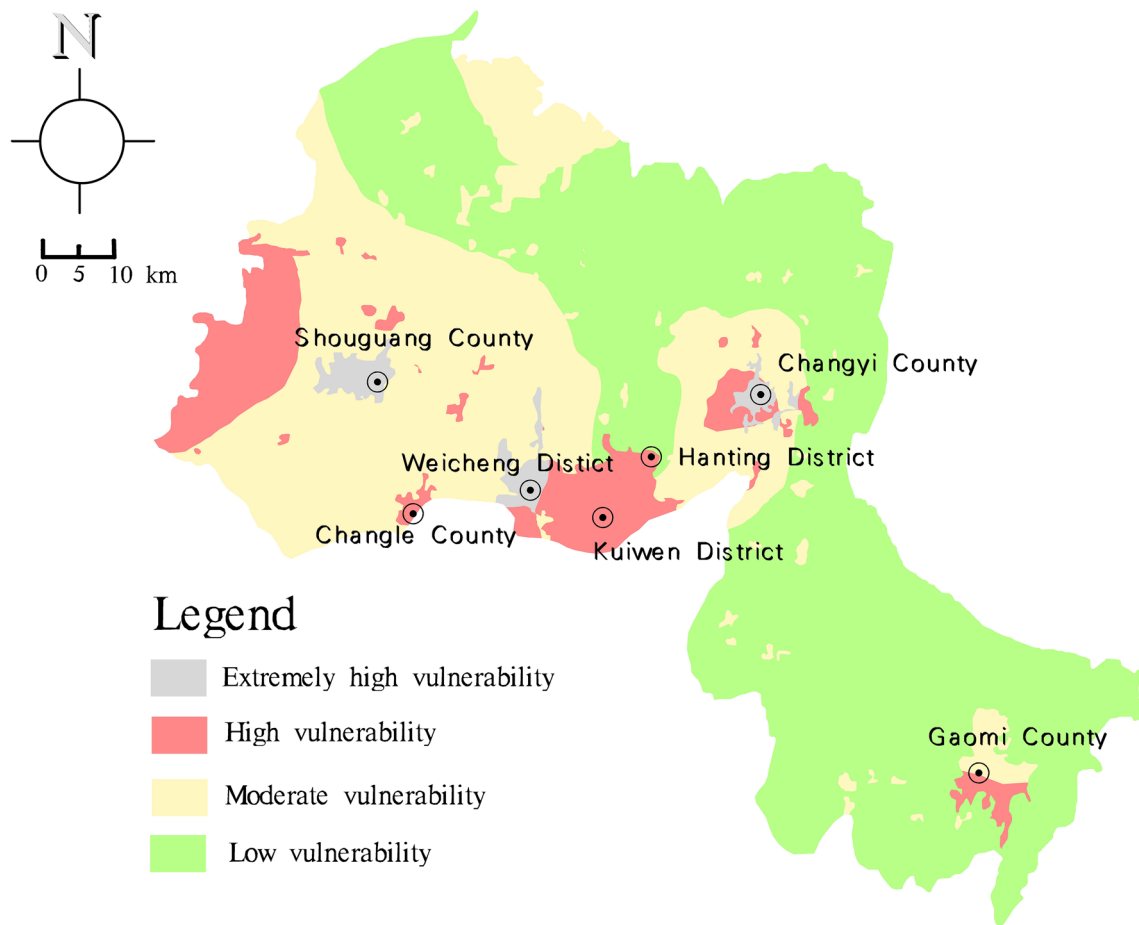


Fig. 9 LSD vulnerability map

Table 7 Grading standard for RSF

RSF	Good (R_A)	General (R_B)	Poor (R_C)
MGE (m^3/km^2)	> 100,000	Neither good RSF nor poor RSF	< 20,000
Water quality	Class III		Class V/shallow aquifers without fresh water

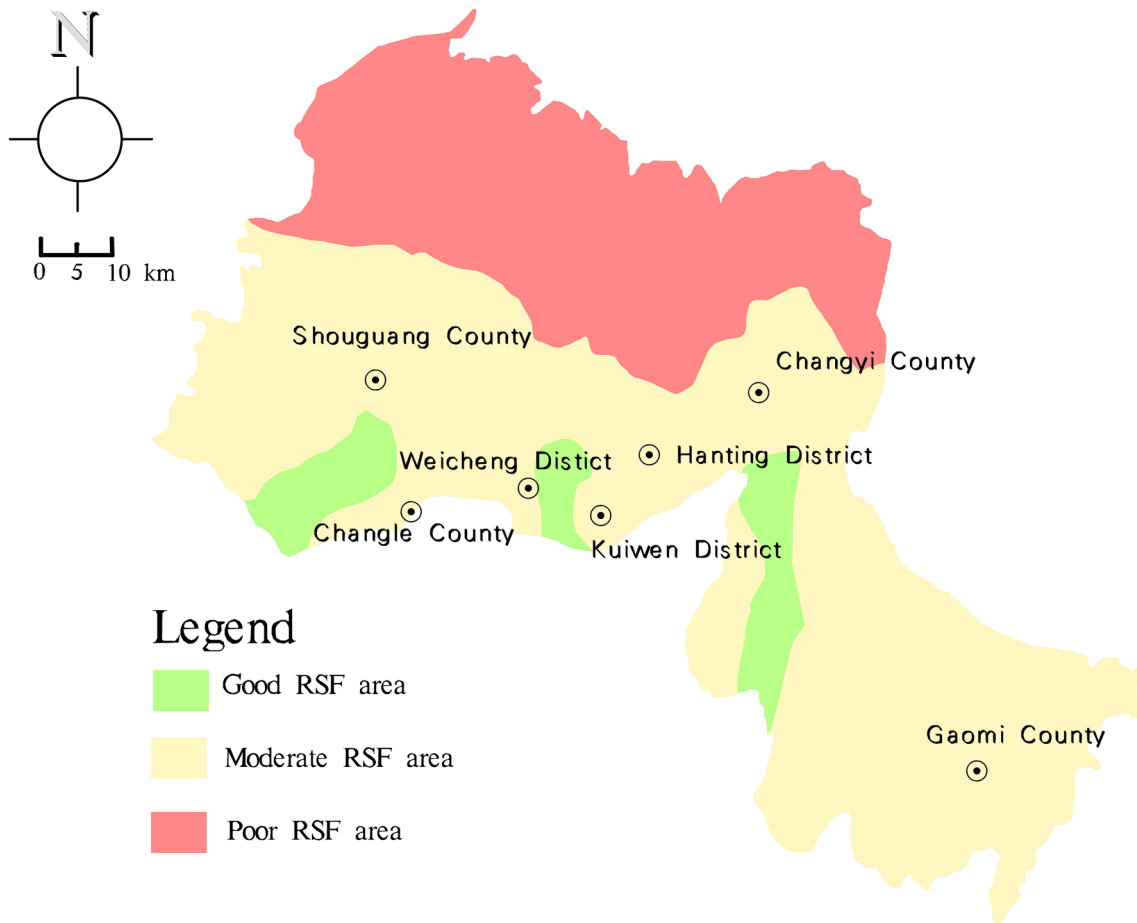


Fig. 10 RSF map

study area is classified as poor RSF, which can slow down the inland migration of the freshwater/saltwater interface.

GSF map

With the vulnerability of two major geo-environmental issues being partitioned according to hydrogeological context and anthropogenic factors, the GSF map provides an objective basis for the site selection of groundwater boreholes. According to the grading standards in Table 8, the GSF of the plain area was divided into four levels.

As shown in the Fig. 11, 45.64% of the plain area falls into the poor GSF area, it concerns nearly half of the area will experience geo-environmental issues if groundwater

Table 8 Grading standard for GSF

GSF	
Poor GSF (G_C)	(SWI OR LSD) high/extremely high vulnerability
General GSF (G_B)	Neither poor GSF nor good GSF
Good GSF (G_A)	(SWI and LSD) low vulnerability

exploitation activities are not restricted. In contrast, 29.46% of the plain area is identified as the good GSF area. This area is mainly distributed in the eastern part of the plain area and in the Hanting District. Concentrated groundwater exploitation may have less impact on the geo-environment

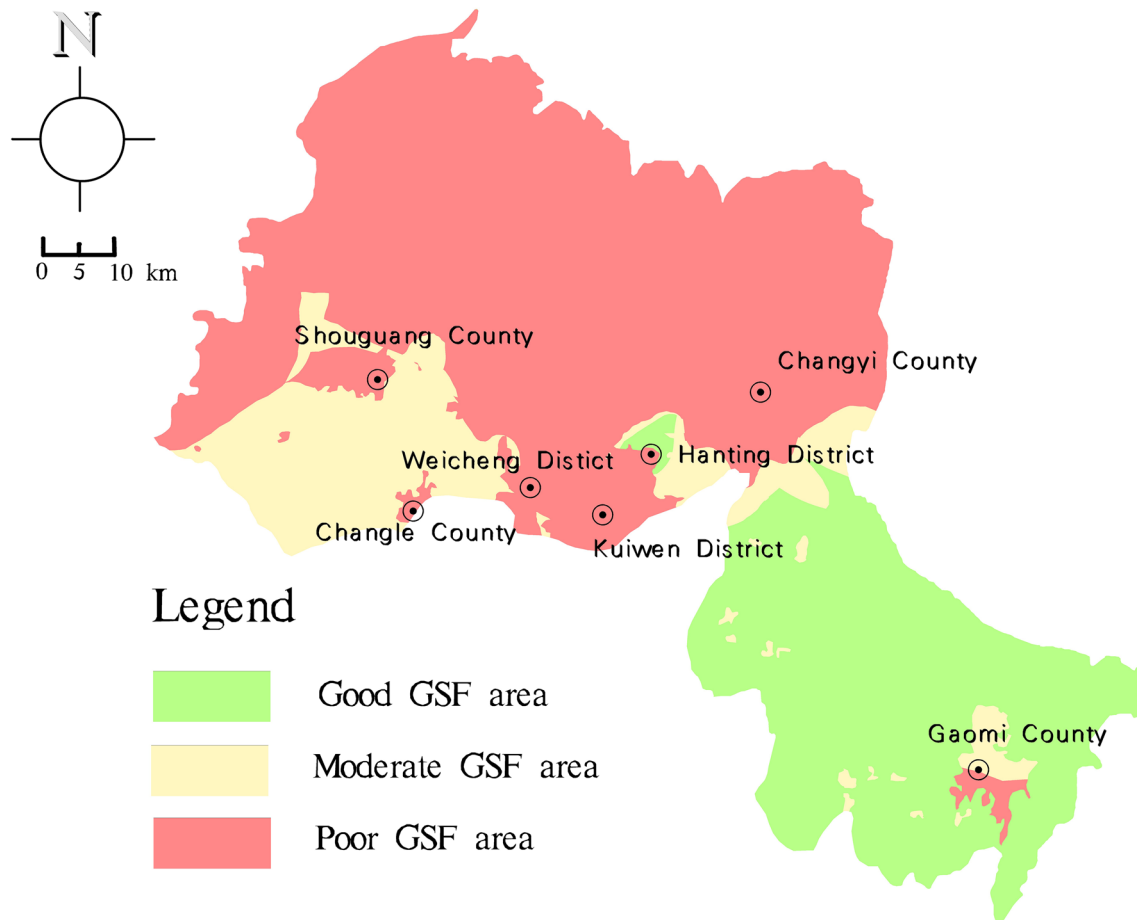


Fig. 11 GSF map

in this area. With regard to moderate GSF areas, small-scale groundwater exploitation is appropriate.

Results of GWFZ

Overlaying the two major function layers of RSF and GSF through the process in Fig. 12a, the GWFZ map was obtained (Fig. 12c). It can be divided into four categories of functional sub-areas in the plain area: concentrated groundwater supply area, decentralized groundwater supply area, vulnerable geo-environment area and unsuitable to exploit groundwater area. With the addition of a type of recharge protection area (hilly area), a total of five categories of functional sub-area have been defined in the study area.

Different types of sub-functional areas should implement different water policies.

1. Concentrated groundwater supply area (1.08% of total area): This functional sub-area is characterized by good RSF and good GSF, and the high-intensity exploitation of groundwater contributes less to the occurrence of regional geo-environmental issues than in other areas.
2. Decentralized groundwater supply area (18.36% of total area): the RSF and GSF in this sub-area have one at a general level (i.e., general RSF or general GSF); this feature indicates that the conditions in this region are insufficient for concentrated groundwater pumping. The water policy in this area, generally speaking, should involve exploitation on a moderate or small scale.
3. Vulnerable geo-environment area (11.78% of total area): poor GSF is the main consideration in this sub-area, and groundwater depression cones caused by high-intensity pumping are difficult to restore in this area, especially in the case of negative hydrological dynamics, which may aggravate SWI and LSD issues. Pumping groundwater from aquifers at small scale is suitable for water management in this sub-area.
4. Unsuitable to exploit groundwater area (14.11% of total area): water resources are poor in this area, and recharge

Due to a sufficient amount of water, the groundwater system readily achieves a balance in water quantity. Water policies in this area should include rational high-density pumping to meet the main drinking water demand in the study area.

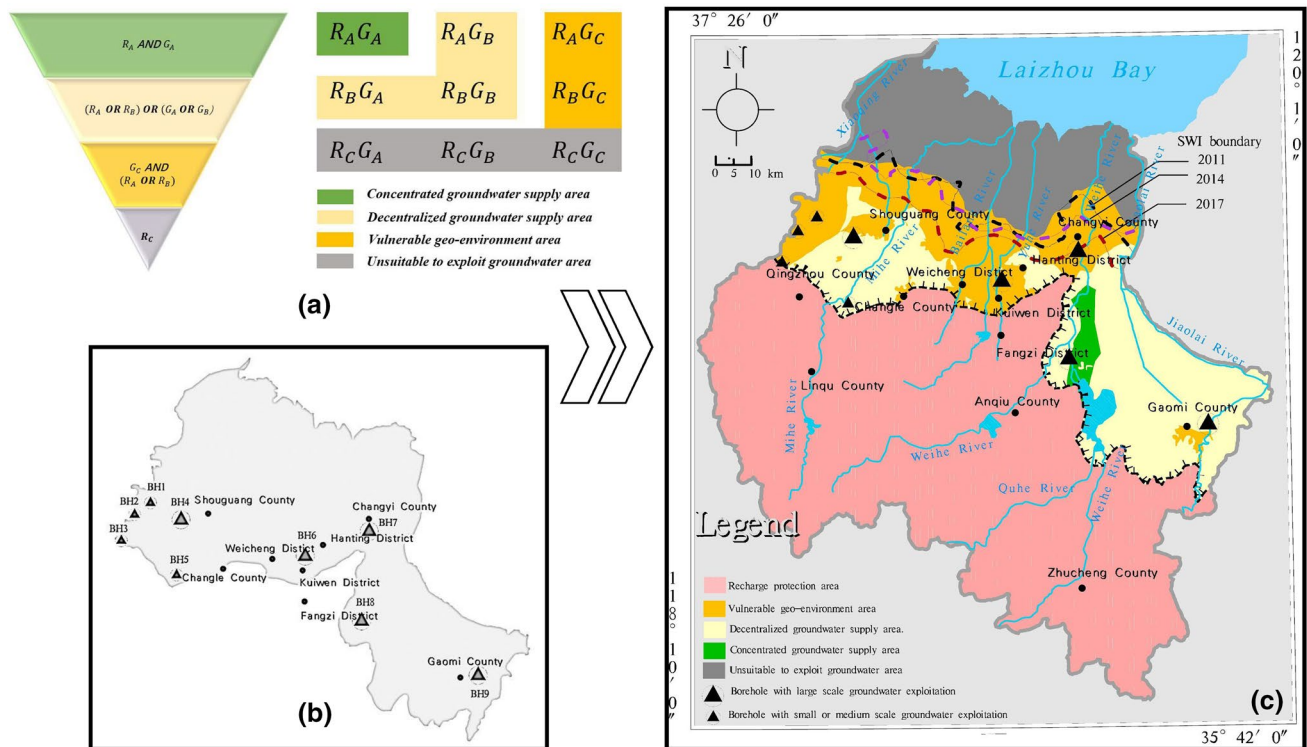


Fig. 12 a Classification criteria for GWFZ; b main boreholes in plain area; c distribution of GWFZ results and SWI boundary from 2011 to 2017 (Guan et al. 2014; Hu et al. 2015; Zhang et al. 2017)

is rather scarce due to poor RSF. This sub-area is mainly associated with shallow aquifers without fresh water in this case study; the exploitation of water resources should be prohibited; the effective ecological measures should be adopted.

5. Recharge protection area (54.67% of total area): in addition to the high cost of exploitation and low water yield of aquifers, the amount of river seepage recharge and lateral runoff recharge account for approximately 1/3 of total recharge, which primarily comes from the hilly areas (Table 5). For these reasons, we classified all hilly areas as recharge protection areas. Groundwater management in hilly areas requires additional precise research, however, which have not been performed in detail in the present study.

Discussion

Integrated water resource planning is essential for groundwater resources to be developed in a sustainable manner (Jothibasu and Anbazhagan 2018). We provide a more detailed GWFZ technique: an indicator-based evaluation system according to a good understanding of the hydrogeological context and anthropogenic factors. The potential area of groundwater, as well as the essential abilities of aquifers

to resist the geo-environmental issues during groundwater exploitation, is highlighted. We chose a typical study area characterized by coastal zones and relying on groundwater supply, as well as the occurrence of groundwater-derived geo-environmental issues. The results of GWFZ are concise and of practical value, providing guidance regarding strategies of groundwater management on a regional scale.

In the present study, the identification of groundwater exploitation potential for RSF is different from that in previous studies (e.g., Kumar et al. 2014; Singh et al. 2018). In particular, the MSE of each hydrogeological unit was used to describe the amount of water, which is applicable to areas where long-term statistics of water exploitation and recharge are available. Regarding the areas that lack historical mining data, the method proposed by Adiat et al. (2012) is also suitable for areas of identifying groundwater exploitation potential. Furthermore, the selection of hydrogeological units with relatively independent recharge sources for statistical analysis still needs to be highlighted. In this paper, the area of the watershed unit is large, which may lead to insufficient accuracy of the evaluation. Delineating smaller catchment units of recharge may contribute to more accurate outputs of GWFZ. In addition, vulnerability assessment is a useful tool for characterizing the essential properties of aquifers against geo-environmental issues caused by groundwater over-exploitation. In fact, the geo-environment issues

driven by groundwater over-exploitation in different regions are dissimilar, such as karst collapse caused by over-pumping in karst aquifers. In this case, the structure of GWFZ can be adjusted according to the realistic situation, while the vulnerability of one or multiple groundwater-derived geo-environmental issues can be superimposed to value the GSF.

Single-parameter sensitivity analysis was employed to analyse the contribution of each parameter to the ALDIT and URT models compared to their theoretical weights (Wu et al. 2018). The effective weights were calculated by the following equation:

$$W = \frac{P_i * P_r}{CI} * 100\%, \tag{4}$$

where *W* is the effective weight of the calculated parameter, *P_i* is the practical rating, *P_r* is the theoretical weight, and *CI* corresponds to each calculated model.

With regard to the ALDIT model, Table 9 indicates that the depth to groundwater above sea level (*L*) and aquifer thickness (*T*) trend to be the most effective indicators of

vulnerability mapping, owing to their effective weights, 32.07 and 16.19%, which are higher than their theoretical weights (26.67 and 16.19%, respectively). The other parameters of the ALDIT model present lower effective weights than the theoretical weights. Additionally, the most effective indicator in the URT model is the thickness of soft soil (*T*), with a theoretical weight of 40% and an effective weight of 48.16%, presenting high effectiveness for LSD vulnerability mapping. To improve the accuracy of the vulnerability model output, some scientific weighting methods can be used, such as ANP (e.g., Baghapour et al. 2016), AHP (e.g., Gorgij and Moghaddam 2016), etc.

However, the root cause of the intensification of SWI in the study area is confirmed to be groundwater over-exploitation (Xue et al. 2000; Han et al. 2014). In the 1980s, large-area depression cones caused by the disorderly exploitation of groundwater have changed regional flow fields (Hu et al. 2015), and SWI was considered a serious geo-environment issue in the study area. In recent years, changes in the SWI boundary have shown that SWI is still progressing (Fig. 12c), demonstrating the relationship with the aforementioned unreasonable groundwater management. Nine primary boreholes (in Fig. 12b) in the plain area (including five boreholes with high actual water production and four boreholes with low-moderate of actual water production) were used to discuss whether they are suitable for mining (Table 10). Five boreholes fall within the poor GSF area, including two boreholes of high actual water production, which significantly accelerate the deterioration of geo-environmental issues. Moreover, BH4 and BH9 need to be carefully analyzed to determine whether the amount of production exceeds the allowed water amount of the local hydrogeological unit.

Overall, the GWFZ method is characterized by simple data acquisition and concise results for groundwater management; thus, it can be applied to other regions. In addition,

Table 9 Single-parameter sensitivity analysis for ALDIT model and URT model

Parameters	Theoretical weights (%)	Effective weights (%)			STD (%)
		Max	Min	Mean	
ALDIT model					
A	20.00	36	6.67	18.76	6.44
L	26.67	55.17	11.11	32.07	10.98
D	26.67	47.06	10.00	19.94	8.58
I	13.33	30.77	4.88	13.03	5.58
T	13.33	44.44	4.17	16.19	9.00
URT model					
U	40.00	72.73	14.29	38.35	11.90
R	20.00	40.00	5.88	13.49	7.52
T	40.00	72.73	18.18	48.16	12.61

Table 10 Boreholes in the study area

Boreholes (BH)	RSF	GSF	Actual water production description	Agreement between expected and actual water production description
BH1	General	Poor	Low–medium	Disagree
BH2	General	Poor	Low–medium	Disagree
BH3	General	Poor	Low–medium	Disagree
BH4	General	General	High	Disagree
BH5	Good	General	Low–medium	Agree
BH6	General	Poor	High	Disagree
BH7	General	Poor	High	Disagree
BH8	Good	Good	High	Agree
BH9	General	General	High	Disagree

High actual water production defined as $\geq 50,000 \text{ m}^3/\text{day}$, while, low–moderate water production defined as $< 50,000 \text{ m}^3/\text{day}$

groundwater management in hilly areas should also be worthy of attention.

Conclusions

This paper discussed coastal groundwater management based on identifying the RSF and GSF to provide a dominant direction to improve the local water policy. The net conclusions were as follows.

1. The framework of GWFZ was divided into two aspects of RSF and GSF to select indicators. The selection of indicators is based on identifying the potential areas of groundwater exploitation for the RSF on the one hand and vulnerability assessments pertaining to typical geo-environmental issues (SWI, LSD) derived by groundwater over-exploitation in the study area for the GSF on the other hand. Hence, a more detailed methodology was provided for GWFZ.
2. GWFZ was applied to divide the study area into five functional sub-areas in the GIS environment: concentrated groundwater supply area (1.08% of total area), decentralized groundwater supply area (18.36%), vulnerable geo-environment area (11.78%), unsuitable to exploit groundwater area (14.11%), and recharge protection area (54.67%). For practical verification, we found that the actual water production amount of a total of seven boreholes in the study area was identified to be unsuitable, which indicates a connection with the inland SWI boundary.
3. Single-parameter sensitivity analysis was employed to identify the most effective weights in both the ALDIT and URT models. For the ALDIT model, it tends to be depth to groundwater above sea Level (L) and aquifer thickness (T), while for the URT model, it is thickness of soft soil (T).

Acknowledgements Funding for this project are supported by National Natural Science Foundation of China (No. 41572212) and Fundamental Research Funds for the Central Universities, China University of Geoscience, Wuhan (No.: CUGCJ1822). The authors thank Linwei SUN, Yonggang LI and Xiaoyu WU for their support and assistance in the analysis of the rationality of zoning. Thanks for the Editor and Reviewers' good comments and hard work.

References

Adiat KAN, Nawawi MNM, Abdullah K (2012) Assessing the accuracy of GIS-based elementary multi criteria decision analysis as a spatial prediction tool—a case of predicting potential zones of sustainable groundwater resources. *J Hydrol* 440–441:75–89

- Allouche N, Maanan M, Gontara M (2017) A global risk approach to assessing groundwater vulnerability. *Environ Modell Softw* 88:168–182
- Baghapour MA, Nobandegani AF, Talebbeydokhti N (2016) Optimization of DRASTIC method by artificial neural network, nitrate vulnerability index, and composite DRASTIC models to assess groundwater vulnerability for unconfined aquifer of Shiraz Plain, Iran. *J Environ Health Sci Eng* 14:13
- Bi QX (2006) Evaluation and study on water environment quality of Weifang City. Hohai University, Nanjing (**in Chinese**)
- Bouderbala A, Remini B, Saaed Hamoudi A, Pulido-Bosch A (2016) Assessment of groundwater vulnerability and quality in coastal aquifers: a case study (Tipaza, North Algeria). *Arab J Geosci* 9:1–12
- CGSB (2017) hydrogeological and geological database. China Geological Survey Bureau. <http://geodata.ngac.cn/>. Accessed Jan 2017
- Chachadi AG (2005) Seawater intrusion mapping using modified GALDIT indicator model - case study in Goa. *Jalvigyan Sameeksha* 20:29–45
- Chen HH, Zhang YX, Wang XM, Ren ZY, Li L (1997) Salt-water intrusion in the lower reaches of the Weihe River, Shandong Province, China. *Hydrogeol J* 5(3):82–88
- Dong DL, Sun WJ, Zhu ZC, Xi S, Lin G (2013) Groundwater risk assessment of the third aquifer in Tianjin City, China. *Water Resour Manag* 27(8):3179–3190
- Gao SD (2005) The estimation of the groundwater resources in Weifang City. Hohai University, Nanjing (**in Chinese**)
- Grogij AD, Moghaddam AA (2016) Vulnerability Assessment of salt-water intrusion using simplified GAPDIT method: a case study of Azarshahr Plain Aquifer, East Azerbaijan, Iran. *Arab J Geosci* 9:106
- Guan QH, Chen XQ, Zhang J (2014) Analysis on dynamic changes of salt water intrusion in Northern Weibei Plain in South Laizhou Bay. *Shandong Land Resour* 9:39–42 (**in Chinese**)
- Han DM, Kohfahl C, Song XF, Xiao GQ (2011) Geochemical and isotopic evidence for palaeo-seawater intrusion into the south coast aquifer of Laizhou Bay, China. *Appl Geochem* 26:863–883
- Han DM, Song XF, Currell MJ, Yang JL (2014) Chemical and isotopic constraints on evolution of groundwater salinization in the coastal plain aquifer of Laizhou Bay, China. *J Hydrol* 508:12–27
- Hu YZ, Li H, Li Y, Shi PX (2015) Hydrogeochemical recognition of seawater intrusion process at the typical profile in Laizhou Bay. *Geol Survey Res* 1:41–50 (**in Chinese**)
- Hu XM, Ma CM, Deng B (2017) Risk evaluation of land subsidence in coastal areas of Jiangsu Province. *Geol Sci Technol Inf* 36(2):222–228 (**in Chinese**)
- Jothibasu A, Anbazhagan S (2018) Hydrogeological assessment of the groundwater aquifers for sustainability state and development planning. *Environ Earth Sci* 77:88
- Kazakis N, Spiliotis M, Voudouris K, Pliakas FK (2018) A fuzzy multicriteria categorization of the GALDIT method to assess seawater intrusion vulnerability of coastal aquifers. *Sci Total Environ* 621:524–534
- Kumar DM, Shah T (2006) Groundwater pollution and contamination in India: the emerging challenge. *IWMI-TATA Water Policy Progr Draft Pap* 1:14
- Kumar T, Gautam AK, Kumar T (2014) Appraising the accuracy of GIS-based multi-criteria decision making technique for delineation of Groundwater potential zones. *Water Resour Manag* 28(13):4449–4466
- Li PY, Wu JH (2010) Groundwater environmental problems and their countermeasures. *Environ Sci Manag* 35(4):60–62 (**in Chinese**)
- Luoma S, Okkonen J, Korkka-Niemi K (2017) Comparison of the AVI, modified SINTACS and GALDIT vulnerability methods under future climate-change scenarios for a shallow low-lying coastal aquifer in southern Finland. *Hydrogeol J* 25(1):203–222

- Mahrez B, Klebingat S, Begacem Houha (2018) GIS-based GALDIT method for vulnerability assessment to seawater intrusion of the Quaternary coastal Collo aquifer (NE-Algeria). *Arab J Geosci* 11:71
- MLR (1994) Groundwater quality standards (GB/T 14848-93). Ministry of Land and Resources, Beijing **(in Chinese)**
- Mogaji KA, Lim HS (2018) Development of groundwater favourability map using GIS-based driven data mining models: an approach for effective groundwater resource management. *Geocarto Int* 33(4):397–422
- Motevalli A, Moradi HR, Javadi S (2018) A Comprehensive evaluation of groundwater vulnerability to saltwater up-coning and sea water intrusion in a coastal aquifer (case study: Ghaemshahr-juybar aquifer). *J Hydrol* 557:753–773
- MWR (2005) Groundwater functional zoning outline. Ministry of Water Resources, Beijing **(in Chinese)**
- Pedreira R, Kallioras A, Pliakas F (2015) Groundwater vulnerability assessment of a coastal aquifer system at River Nestos eastern Delta, Greece. *Environ Earth Sci* 73(10):6387–6415
- Recinos N, Kallioras A, Pliakas F (2015) Application of GALDIT index to assess the intrinsic vulnerability to seawater intrusion of coastal granular aquifers. *Environ Earth Sci* 73:1017–1032
- SDHB (2013) Report on the evaluation of groundwater overexploitation area in Shandong Province. Shandong Hydrological Bureau, Jinan **(in Chinese)**
- SDSB (2018) Statistical yearbook of Shandong Province, Shandong Statistics Bureau. <http://www.stats-sd.gov.cn/col/col6279/index.html>. **(in Chinese)**
- Singh LK, Jha MK, Chowdary VM (2018) Assessing the accuracy of GIS-based multi-criteria decision analysis approaches for mapping groundwater potential. *Ecol Indic* 91:24–37
- Sun QY, Yu XX, Hu SP (2008) Extraction and application of hydrological information based on DEM in ArcGIS environment. *J Beijing For Univ* 30:144–147 **(in Chinese)**
- Wang YY, Sun Q, Tan RJ (2009) Land subsidence in coastal areas based on geological factors. *Chinese J Geol Hazard Control* 4:86–94 **(in Chinese)**
- Wang JJ, He JT, Chen HH (2012) Assessment of groundwater contamination risk using hazard quantification, a modified DRASTIC model and groundwater value, Beijing Plain, China. *Sci Total Environ* 432:216–226
- Wu XY, Li B, Ma CM (2018) Assessment of groundwater vulnerability by applying the modified DRASTIC model in Beihai City, China. *Environ Sci Pollut R* 25:12713–12727
- Xue YQ, Wu JC, Xie CH, Zhang YX (1997) Study on intrusion of sea and salt water along Laizhou Bay. *Chin Sci Bull* 22:2360–2368 **(in Chinese)**
- Xue YQ, Wu JC, Ye SJ, Zhang YX (2000) Hydrogeological and hydrogeochemical studies for salt water intrusion on the south coast of Laizhou Bay, China. *Groundwater* 38(1):38–45
- Yang JX (1991) Distribution patterns of soft soil layers and the classification of engineering geology layers in Tianjin plain. *J Tianjin Univ* S2:126–131 **(in Chinese)**
- Yang Y, Zheng FD, Liu LC (2013) Susceptibility zoning and control measures on land subsidence caused by groundwater exploitation. *Geol China* 40(2):653–658 **(in Chinese)**
- Zhang RQ, Liang X, Jin MG (2011) Fundamentals of hydrogeology. Geological Press, Beijing **(in Chinese)**
- Zhang YW, Li HX, Shang TT (2016) Application of extenics theory for partition of land subsidence susceptible area of Dezhou City based on analytic hierarchy process. *Shandong Land Resour* 32(7):58–64 **(in Chinese)**
- Zhang X, Miao J, Hu BX (2017) Hydrogeochemical characterization and groundwater quality assessment in intruded coastal brine aquifers (Laizhou Bay, China). *Environ Sci Pollut Res* 24:21073–21090
- Zheng YM, Gao MS, Liu S, Wang ST (2014) Distribution characteristics of subsurface brine resources on the southern coast of Laizhou bay since late Pleistocene. *Hydrogeol Eng Geol* 41(5):11–18 **(in Chinese)**

Publisher's Note Springer Nature remains neutral with regard to jurisdictional claims in published maps and institutional affiliations.